49th AIAA Aerospace Sciences Meeting including the New Horizons Forum and Aerospace Exposi
4 - 7 January 2011, Orlando, Florida

Unsteady Adjoint Method for the Optimal Control of Advection and Burger's Equations using High-Order Spectral Difference Method

K. Ou* and A. Jameson †

Aeronautics and Astronautics Department, Stanford University, Stanford, CA 94305

In this study, we investigate the method for adjoint-based optimal control of linear and non-linear equations. In particular, we are interested in the formulation of the unsteady adjoint method based on the high-order spectral difference method. For the linear equation, we consider the simple 1D advection equation. For the non-linear equation, we consider the 1D viscous Burger's equation. In both cases, the inverse design of the target solution is achieved through control of the initial condition. The focus of the study is the formulation of the unsteady adjoint method using the high-order spectral difference method. The paper demonstrates that the minimal numerical dissipation inherent in the high order method is very beneficial for adjoint type problem where backward integration in time is involved. The combination of adjoint approach and high order method will lead to an useful tool for optimization in the field of aeroacoustic simulation and design.

I. Introduction

While much work has been done in the field of steady adjoint approach for optimal control and inverse design problems using traditional CFD methods[1–4] such as finite volume methods, the current trend and demand for more time-accurate and spatial-accurate methods entail further development of the adjoint-based approach. Recent research has seen the combination of the unsteady adjoint method with the high order methods such as the Discontinous Galerkin (DG) method.[5–7] Method of this type can be a significant aid to the field of aeroacoustic design and optimization, since the capture of acoustic signiture often requires the time-accuracy and spatial-accuracy of the high order methods which have very small numerical dissipations. In this study, we investigate the formulation of unsteady adjoint approach based on high-order spectral difference (SD) method, and explore methods that can lead to better computational and optimization efficiency. We consider the problems of the optimal control of the advection and Burger's equations, by treating the initial conditions as the control inputs, and matching the final solutions with design target profiles.

II. High-Order Spectral Difference Method

The SD method, like DG, is element-wise continuous. Within each individual element, collocated solution and flux points are used to store values of the flow solution and flux respectively. With these solution and flux points, one solution polynomial and one flux polynomial can be constructed to represent the flow solution and flux in the local domain span by the element. The flux polynomial is one order higher than the solution polynomial such that when it is differentiated the flux divergence is of the same order as the solution polynomial. Therefore, the number of flux points is one more than that of solution points. At the element interface, where two sets of local solution meet each other, the flux across the interface is discontinuous. A single valued numerical flux is computed by solving a Riemann problem. Details of the SD formulation are outlined in the subsequent section. The standard SD method follows the work by Sun etc.[8]

*PhD Candidate, Aeronautics and Astronautics Department, Stanford University, AIAA Student Member.
†Thomas V Jones Professor, Aeronautics and Astronautics Department, Stanford University, AIAA Fellow.

II.A. Affine Transformation

Consider the unsteady 1D model equation of the form

$$\frac{\partial u}{\partial t} + \frac{\partial f^i}{\partial x} + \frac{\partial f^v}{\partial x} = 0 \tag{1}$$

where u is the solution variable, and f^i and f^v are the inviscid and viscous flux vectors. To achieve an efficient implementation, all elements in the physical domain $[a, b]$ are transformed into a standard unit element ($0 \leq \xi \leq 1$). The Jacobian of the transformation can be computed. The governing equations in the physical domain are then transferred into the computational domain, and the transformed equations take the following form:

$$\frac{\partial \tilde{u}}{\partial t} + \frac{\partial \tilde{f}^i}{\partial \xi} + \frac{\partial \tilde{f}^v}{\partial \xi} = 0 \tag{2}$$

where $\tilde{u} = |J| \cdot u$ and $\tilde{f}^i = |J| \cdot f^i$ and $\tilde{f}^v = |J| \cdot f^v$.

II.B. Solution and Flux Basis Functions

In the standard element, two sets of points are defined, namely the solution points and the flux points. In order to construct a degree $(N-1)$ polynomial in each coordinate direction, solution at N points are required. The solution points in 1D are chosen to be the Chebyshev points defined by:

$$X_s = \frac{1}{2}\left[1 - cos\left(\frac{2s-1}{2N} \cdot \pi\right)\right], s = 1, 2, \cdots, N. \tag{3}$$

The flux points were selected to be the Legendre-Gauss quadrature points plus the two end points 0 and 1, as suggested by Huynh.[9] Choosing $P_{-1}(\xi) = 0$ and $P_0(\xi) = 1$, the higher-degree Legendre polynomials are

$$P_n(\xi) = \frac{2n-1}{n}(2\xi - 1)P_{n-1}(\xi) - \frac{n-1}{n}P_{n-2}(\xi) \tag{4}$$

The locations of these Legendre-Gauss quadrature points are the roots of equations $P_n(\xi) = 0$. The choice of this particular set of flux points leads to energy stable SD scheme, as recently proven by Jameson.[10] Using the solutions at N solution points, a degree $(N-1)$ polynomial can be built using the following Lagrange basis defined as:

$$h_i(X) = \prod_{s=1, s\neq i}^{N}\left(\frac{X - X_s}{X_i - X_s}\right) \tag{5}$$

Similarly, using the fluxes at $(N+1)$ flux points, a degree N polynomial can be built for the flux using a similar Lagrange basis as:

$$l_{i+1/2}(X) = \prod_{s=0, s\neq i}^{N}\left(\frac{X - X_{s+1/2}}{X_{i+1/2} - X_{s+1/2}}\right) \tag{6}$$

The reconstructed solution in the unit element is,

$$u(\xi) = \sum_{i=1}^{N} \frac{\tilde{u}_i}{|J_i|} h_i(\xi) \tag{7}$$

Similarly, the reconstructed flux polynomials take the following form:

$$\begin{aligned} \tilde{f}^i(\xi) &= \sum_{i=0}^{N} \tilde{f}^i{}_{i+1/2} l_{i+1/2}(\xi), \\ \tilde{f}^v(\xi) &= \sum_{i=0}^{N} \tilde{f}^v{}_{i+1/2} l_{i+1/2}(\xi) \end{aligned} \tag{8}$$

The reconstructed fluxes are only element-wise continuous, but discontinuous across cell interfaces. For the inviscid flux, a common numerical flux, such as upwind or central flux, at interface is computed to ensure conservation and stability.

II.C. Procedure for Inviscid Residual Computation

In summary, the algorithm to compute the inviscid flux derivatives consists of the following steps:

1. Given the solution variable at the solution points, the solution variable is computed at the flux points and the inviscid fluxes at the interior flux points can be determined.
2. The inviscid fluxes at the element interfaces are computed using common numerical flux.
3. The derivatives of the fluxes are computed at the solution points using the derivatives of Lagrange operators l

$$\left(\frac{\partial \tilde{f}^i}{\partial \xi}\right)_i = \sum_{r=0}^{N} \tilde{f^i}_{r+1/2} \cdot l'_{r+1/2}(\xi_i) \tag{9}$$

II.D. Procedure for Viscous Residual Computation

The procedures to get the viscous fluxes can be described as the following steps:

1. reconstruct u_{fp} at the flux points from the conservative variables at the solution points using equation (7).
2. average the field of u_{fp} on the element interfaces as $\overline{u}_{fp} = \frac{1}{2}(u^L_{fp} + u^R_{fp})$. For interior flux points, $\overline{u}_{fp} = u_{fp}$. Meanwhile, appropriate boundary conditions shall be applied for specific edge flux points.
3. evaluate ∇u at solution points from $\overline{u}_{fp}$ using equation (9) where $\nabla u = u_x$ and $u_x = \frac{\partial u}{\partial \xi} \cdot J$.
4. reconstruct ∇u from solution points to flux points and using equation (7), average them on the element interfaces as $\overline{\nabla u}_{fp} = \frac{1}{2}(\nabla u^L_{fp} + \nabla u^R_{fp})$
5. use $\overline{u}_{fp}$ and $\overline{\nabla u}_{fp}$ in order to compute the viscous flux vectors at the element interfaces.

III. Formulation of Design Optimization

The application of control theory to design optimization problem has helped to circumvent the large computation cost of the traditional finite difference approach with large number of design variables. With the solution of the adjoint equation, the gradient can be determined with roughly the computational cost of two flow solutions, independently of the number of design variables. The key ideas of this section follows the work by Jameson,[11]

III.A. Control Theory Approach to the Design Problem

Define a cost function

$$I = \int_{\mathcal{B}} (u - u_d)^2 d\mathcal{B}$$

The boundary $\mathcal{B}$ is now treated as the control, which is varied in order to minimize the cost I, subject to the constraint that the governing equation is satisfied in the compuational domain.

Linear Advection Equation

For 1D linear advection equation spanning [a,b], the cost function is

$$I = \int_a^b (u - u_d)^2 dx$$

The governing equation is

$$\frac{\partial u}{\partial t} + a\frac{\partial u}{\partial x} = 0$$

The initial condition, which is also the control input, is

$$u(x,0) = f(x)$$

Therefore the initial profile $f(x)$, which spans the entire flow domain [a,b], is now treated as the control, which is varied in order that the final solution profile u matches the design solution profile u_d, subject to the satisfaction of the linear advection equation.

Burger's Equation

For 1D nonlinear Burger's equation spanning [a,b], the cost function is

$$I = \int_a^b (u - u_d)^2 dx$$

The governing equation is

$$\frac{\partial u}{\partial t} + u\frac{\partial u}{\partial x} - \mu\frac{\partial^2 u}{\partial x^2} = 0$$

The initial condition, as well as the control input, is

$$u(x,0) = f(x)$$

Therefore the initial profile $f(x)$, which spans the entire flow domain [a,b], is now treated as the control, which is varied in order that the final solution profile u matches the design solution profile u_d, subject to the satisfaction of the nonlinear Burger's equation.

III.B. Formulation of Optimal Design Problem

Finite Difference Approach to Optimal Design

Define the control input through a set of design parameters to be the weights α_i applied to a set of shape functions $b_i(x)$ so that the control profile is represented as

$$f(x) = \sum \alpha_i b_i(x).$$

Then a cost function I is selected to be the difference between the actual and the design target profile, and I is regarded as a function of the parameters α_i. The sensitivities $\frac{\partial I}{\partial \alpha_i}$ may now be estimated by making a small variation $\delta\alpha_i$ in each design parameter in turn and recalculating the flow to obtain the change in I. Then

$$\frac{\partial I}{\partial \alpha_i} \approx \frac{I(\alpha_i + \delta\alpha_i) - I(\alpha_i)}{\delta\alpha_i}.$$

The gradient vector $\mathcal{G} = \frac{\partial I}{\partial \alpha}$ may now be used to determine a direction of improvement. The simplest procedure is to make a step in the negative gradient direction by setting

$$\alpha^{n+1} = \alpha^n + \delta\alpha,$$

where

$$\delta\alpha = -\lambda\mathcal{G}$$

so that to first order

$$I + \delta I = I - \mathcal{G}^T\delta\alpha = I - \lambda\mathcal{G}^T\mathcal{G} < I$$

The main disadvantage of this approach is the need for a number of flow calculations proportional to the number of design variables to estimate the gradient. The computational costs can thus become prohibitive as the number of design variables is increased.

Adjoint Approach to Optimal Design

For the 1D advection or Burger's equation, the final solution profile, which we aim to design to match u_d, are functions of the flow-field variable u and the initial condition, which may be represented by the function f, say. Then

$$I = I\left(u, f\right),$$

and a change in f results in a change

$$\delta I = \left[\frac{\partial I^T}{\partial u}\right] \delta u + \left[\frac{\partial I^T}{\partial f}\right] \delta f \tag{10}$$

in the cost function. Suppose that the governing equation R which expresses the dependence of u and f within the flowfield domain D can be written as

$$R\left(u, f\right) = 0. \tag{11}$$

Then δu is determined from the equation

$$\delta R = \left[\frac{\partial R}{\partial u}\right] \delta u + \left[\frac{\partial R}{\partial f}\right] \delta f = 0. \tag{12}$$

Since the variation δR is zero, it can be multiplied by a Lagrange Multiplier ψ and subtracted from the variation δI without changing the result. Thus equation (10) can be replaced by

$$\begin{aligned} \delta I &= \frac{\partial I^T}{\partial u}\delta u + \frac{\partial I^T}{\partial f}\delta f - \psi^T \left(\left[\frac{\partial R}{\partial u}\right] \delta u + \left[\frac{\partial R}{\partial f}\right] \delta f \right) \\ &= \left\{ \frac{\partial I^T}{\partial u} - \psi^T \left[\frac{\partial R}{\partial u}\right] \right\} \delta u + \left\{ \frac{\partial I^T}{\partial f} - \psi^T \left[\frac{\partial R}{\partial f}\right] \right\} \delta f. \end{aligned} \tag{13}$$

Choosing ψ to satisfy the adjoint equation

$$\left[\frac{\partial R}{\partial u}\right]^T \psi = \frac{\partial I}{\partial u} \tag{14}$$

the first term is eliminated, and we find that

$$\delta I = \mathcal{G}^T \delta f, \tag{15}$$

where

$$\mathcal{G} = \frac{\partial I^T}{\partial f} - \psi^T \left[\frac{\partial R}{\partial f}\right].$$

The advantage is that (15) is independent of δu, with the result that the gradient of I with respect to an arbitrary number of design variables can be determined without the need for additional flow-field evaluations. In the case that (11) is a partial differential equation, the adjoint equation (14) is also a partial differential equation and appropriate boundary conditions need to be determined. Once the gradient $\mathcal{G}$ has been determined an improvement can be obtained by making a shape change

$$\delta f = -\lambda \mathcal{G} \tag{16}$$

where λ is sufficiently small and positive so that

$$\delta I = -\lambda \mathcal{G}^T \mathcal{G} \quad < 0$$

Optimization Procedure

The design procedure can be summarized as follows:

1. Solve the flow equations $R = \frac{\partial u}{\partial t} + a\frac{\partial u}{\partial x} = 0$ or $R = \frac{\partial u}{\partial t} + u\frac{\partial u}{\partial x} - \mu\frac{\partial^2 u}{\partial x^2} = 0$ for u
2. Solve the adjoint equations $\left[\frac{\partial R}{\partial u}\right]^T \psi = \frac{\partial I}{\partial u}$ for ψ subject to appropriate boundary conditions.
3. Evaluate $\mathcal{G} = \frac{\partial I^T}{\partial f} - \psi^T \left[\frac{\partial R}{\partial f}\right]$.
4. Update the shape based on the direction of steepest descent $\delta f = -\lambda \mathcal{G}$.
5. Return to 1 until convergence is reached.

IV. Continuous Adjoint Methods

The continuous adjoint theory was developed by combining the variation of the cost function and flow equation with respect to the flow variables and desgin variables through the use of Lagrange multipliers or adjoint variables. Collecting the terms associated with the variation of the flow variables produces the adjoint equation and its boundary condition. The terms associated with the variation of the design variable produce the gradient.[12] Following this general approach, the derivations of the continuous adjoint for the advection and viscous Burgers equations are outlined in the following sections.

IV.A. Advection Equation

To derive the continuous adjoint equation, we consider a constrained optimization problem by augmenting the original optimization cost function with the constraint (the flow equation) through a Lagrange multipliter as follows.

Theory of Lagrange Multiplier

According to the theory of Lagrange multipliers,

$$I' - < R, \psi >' = 0$$

Now take the variation of the cost function with respect to the state variable, noting that a variaton of the initial condition causes a variation δu or u' in the flow variable, we have

$$I' = \frac{1}{2}\int_a^b (u_f - u_d)\ u'\ dx$$

Next we form a L^2-inner product of the advection equation R and the adjoint variable ψ as follows

$$< R, \psi > = \int_0^T \int_a^b (\frac{\partial u}{\partial t} + a\frac{\partial u}{\partial x})\ \psi\ dx\ dt$$

The variation of $< R, \psi >$ with respect to the variable u can be written as

$$< R, \psi >' = \int_0^T \int_a^b (\frac{\partial u'}{\partial t} + a\frac{\partial u'}{\partial x})\ \psi\ dx\ dt = \int_0^T \int_a^b (\frac{\partial u'}{\partial t}\ \psi)\ dx\ dt + \int_0^T \int_a^b (a\frac{\partial u'}{\partial x}\ \psi)\ dx\ dt$$

This can be integrated by parts to arrive at

$$< R, \psi >' = \int_a^b (u' \left[\psi\right]_0^T)\ dx - \int_0^T \int_a^b (u'\frac{d\psi}{dt})\ dx\ dt + \int_0^T (a\psi \left[u'\right]_a^b)\ dt - \int_0^T \int_a^b (au'\frac{d\psi}{dx})\ dt\ dx$$

Rearrange to get

$$< R, \psi >' = -\int_0^T \int_a^b (u'\frac{d\psi}{dt})\ dx\ dt - \int_0^T \int_a^b (au'\frac{d\psi}{dx})\ dx\ dt + \int_a^b (u' \left[\psi\right]_0^T)\ dx + \int_0^T (a\psi \left[u'\right]_a^b)\ dt$$

The first two terms can be further combined to obtain

$$< R, \psi >' = \int_0^T \int_a^b (-\frac{\partial \psi}{\partial t} - a\frac{\partial \psi}{\partial x})\ u'\ dx\ dt + \int_a^b (u'\ \left[\psi\right]_0^T)\ dx + \int_0^T (a\psi\ \left[u'\right]_a^b)\ dt$$

The augmented cost function $I' - < R, \psi >' = 0$ can now be written in full as

$$\left[\frac{1}{2}\int_a^b (u_f - u_d)\ u'\ dx\right]_A + \left[\int_0^T \int_a^b (\frac{\partial \psi}{\partial t} + a\frac{\partial \psi}{\partial x})\ u'\ dx\ dt\right]_B - \left[\int_a^b (u'\ \left[\psi\right]_0^T)\ dx\right]_C - \left[\int_0^T (a\psi\ \left[u'\right]_a^b)\ dt\right]_D = 0$$

The above equation can be satisfied by the satisfaction of the adjoint equation and appropriate boundary and terminal conditions, as outlined in the following.

Adjoint Equation and Its Terminal and Boundary Conditions

The adjoint equation, which eliminates B, is given by:

$$\frac{\partial \psi}{\partial t} + a\frac{\partial \psi}{\partial x} = 0$$

The terminal condition, which eliminates A and C, is given by:

$$\psi(x, T) = \frac{1}{2}(u_f - u_d)$$

The boundary conditions, which eliminates D, are given by:

$$\psi(a, t) = 0$$

$$\psi(b, t) = 0$$

IV.B. Burger's Equation

To derive the continuous adjoint equation, we consider a constrained optimization problem by augmenting the original optimization cost function with the constraint (the flow equation) through a Lagrange multipliter as follows.

Theory of Lagrange Multiplier

According to the theory of Lagrange multipliers,

$$I' - < R, \psi >' = 0$$

Now take the variation of the cost function with respect to the state variable, noting that a variaton of the initial condition causes a variation δu or u' in the flow variable,

$$I' = \frac{1}{2}\int_a^b (u_f - u_d)\ u'\ dx$$

Next we form a L^2-inner product of the Burgers equation R and the adjoint variable ψ as follows

$$< R, \psi > = \int_0^T \int_a^b (\frac{\partial u}{\partial t} + u\frac{\partial u}{\partial x} - \mu\frac{\partial^2 u}{\partial x^2})\ \psi\ dx\ dt$$

The variation of $< R, \psi >$ with respect to the variable u can be written as

$$< R, \psi >' = \int_0^T \int_a^b (\frac{\partial u'}{\partial t}\ \psi)\ dx\ dt + \int_0^T \int_a^b (\frac{\partial u' u}{\partial x}\ \psi)\ dx\ dt - \int_0^T \int_a^b (\mu\frac{\partial^2 u'}{\partial x^2}\ \psi)\ dx\ dt$$

This can be integrated by parts to arrive at, for the first term

$$\int_0^T \int_a^b (\frac{\partial u'}{\partial t}\ \psi)\ dx\ dt = \int_a^b (\left[\psi\ u'\right]_a^b)\ dx - \int_0^T \int_a^b (u'\ \frac{\partial \psi}{\partial t})\ dx\ dt$$

for the second term

$$\int_0^T \int_a^b (\frac{\partial u'u}{\partial x}\ \psi)\ dx\ dt = \int_0^T (\Big[\psi u'u\Big]_a^b)\ dt - \int_0^T \int_a^b (u'u\ \frac{\partial \psi}{\partial x})\ dx\ dt$$

for the third term

$$\int_0^T \int_a^b (\mu\frac{\partial^2 u'}{\partial x^2}\ \psi)\ dx\ dt = \int_0^T (\Big[\mu\psi\frac{\partial u'}{\partial x}\Big]_a^b)\ dt - \int_0^T \int_a^b (\mu\frac{\partial u'}{\partial x}\ \frac{\partial \psi}{\partial x})\ dx\ dt$$

the last term of the third term can be further integrated by parts

$$\int_0^T \int_a^b (\mu\frac{\partial u'}{\partial x}\ \frac{\partial \psi}{\partial x})\ dx\ dt = \int_0^T (\Big[\mu\ \frac{\partial \psi}{\partial x}u'\Big]_a^b)\ dt - \int_0^T \int_a^b (\mu u'\ \frac{\partial^2 \psi}{\partial x^2})\ dx\ dt$$

Combining all four terms and rearranging the equation into a group involving boundary integrals and a group without, the expression for $< R, \psi >'$ becomes

$$\begin{aligned} < R, \psi >' = &- \int_0^T \int_a^b (\frac{\partial \psi}{\partial t} + u\frac{\partial \psi}{\partial x} + \mu\frac{\partial^2 \psi}{\partial x^2})u'\ dx\ dt \\ &+ \int_a^b (\Big[\psi\ u'\Big]_a^b)\ dx + \int_0^T (\Big[\psi u'u\Big]_a^b)\ dt - \int_0^T (\Big[\mu\psi\frac{\partial u'}{\partial x}\Big]_a^b)\ dt + \int_0^T (\Big[\mu\ \frac{\partial \psi}{\partial x}u'\Big]_a^b)\ dt \end{aligned}$$

The augmented cost function $I' - < R, \psi >' = 0$ can now be written in full as

$$\begin{aligned} &\Big[\frac{1}{2}\int_a^b (u_f - u_d)\ u'\ dx\Big]_A + \Big[\int_0^T \int_a^b (\frac{\partial \psi}{\partial t} + u\frac{\partial \psi}{\partial x} + \mu\frac{\partial^2 \psi}{\partial x^2})u'\ dx\ dt\Big]_B - \Big[\int_a^b (\Big[\psi\ u'\Big]_a^b)\ dx\Big]_C \\ &- \Big[\int_0^T (\Big[\psi u'u\Big]_a^b)\ dt\Big]_D + \Big[\int_0^T (\Big[\mu\psi\frac{\partial u'}{\partial x}\Big]_a^b)\ dt\Big]_E - \Big[\int_0^T (\Big[\mu\ \frac{\partial \psi}{\partial x}u'\Big]_a^b)\ dt\Big]_F = 0 \end{aligned}$$

The above equation can be satisfied by the satisfaction of the adjoint equation and appropriate boundary and terminal conditions, as outlined in the following.

Adjoint Equation and Its Terminal and Boundary Conditions

The adjoint equation, which eliminates B, is given by:

$$\frac{\partial \psi}{\partial t} + u\frac{\partial \psi}{\partial x} + \mu\frac{\partial^2 \psi}{\partial x^2} = 0$$

The terminal condition, which eliminates A and C, is given by:

$$\psi(x, T) = \frac{1}{2}(u_f - u_d)$$

The boundary conditions, which eliminates D, E and F, are given by:

$$\psi(a, t) = 0$$

$$\psi(b, t) = 0$$

$$u\psi(b, t) + \mu\frac{\partial \psi(b, t)}{\partial x} = 0$$

V. Numerical Method for the Continuous Adjoint Equations

The flow equation and the adjoint equation with its boundary conditions must be discretized to obtain numerical solutions. The time is discretized with 5-stage fourth order explicit Runge-Kutta method. The space is discretized using Spectral Difference method.

Advection Equation with SD method

We use the SD method outlined in the previous section to discretize both the primal advection equation and its adjoint equation. The primal equation can be discretized using SD method by letting $Q = u$ and $F(u) = au$. The adjoint equation can be discretized using SD method by setting $Q = \psi$ and $F(\psi) = a\psi$.

Burgers Equation with SD method

We use the SD method outlined in the previous section to discretize both the primal Burgers equation and its adjoint equation. The primal equation can be discretized using SD scheme by letting $Q = u$, $F^i(u) = \frac{1}{2}u^2$, and $F^v(u_x) = +\mu\frac{\partial u}{\partial x}$. The adjoint equation can be discretized using SD scheme by letting $Q = \psi$, $F^i(\psi) = u\psi$, and $F^v(\psi_x) = -\mu\frac{\partial \psi}{\partial x}$.

VI. Numerical Results

VI.A. Linear Inviscid Problem I

For the linear inviscid problem, we consider the inverse design of the linear advection equation. Starting with an arbitrary initial condition, we want to obtain a desired final solution distribution. This is achieved through optimal control of the initial condition, which is driven by the adjoint equation. Since we do not consider the control of the boundary conditions, in all cases, the exact boundary conditions are prescribed. The cost function is measured as one half the Euclidean norm of the error between the exact final solution and the actual final solution. A tolerance is specified as $1.0E^{-4}$.

Computational Setup for Linear Advection Equation

Consider the governing equation for linear advection:

$$\frac{du}{dt} + c\frac{\partial u}{\partial x} = 0 \tag{17}$$

One exact solution is:

$$u = e^{-20(x-ct)^2}$$

with periodical boundary condition and the initial solution:

$$u = e^{-20x^2}$$

The computational domain spans $[-10, 10]$ with a total number of 100 elements. The number of solution points witin each element is 4, corresponding to the 4^{th} order accurate SD method. The computation is run with a fixed time step of $dt = 0.05$ until a final time $T = 5$. The same time step size is used for solving the adjoint equation. The convection speed c is equal to 1.

Design Convergence

Firstly we define the final design solution distribution, $u_d(T)$, at a specific final time, T, as:

$$u_d(T) = e^{-20(x-cT)^2}$$

Secondly we specify an abritary initial condition, with the only requirements that no errors at the boundaries, either Dirichilet or Neumann type, are introduced. We set the initial condition as the exact initial condition scaled with a 5^{th} order polynomial as follows:

$$u = e^{-20x^2} + x^5 e^{-20x^2}$$

This is the effectively the exact initial condition with an added disturbance term. We aim to elminate the error source, recover the exact initial condition and attain the final design solution within the specified tolerance. Other more aggressive initial conditions can be used. We present another example in the subsequent section. For the current problem, the convergence of the cost function is shown in figure 1. Very rapid convergence is observed. We obtain the design final solution in only 6 iterations. In fact, it takes only 2 iterations to nearly recover the desired solution distribution.

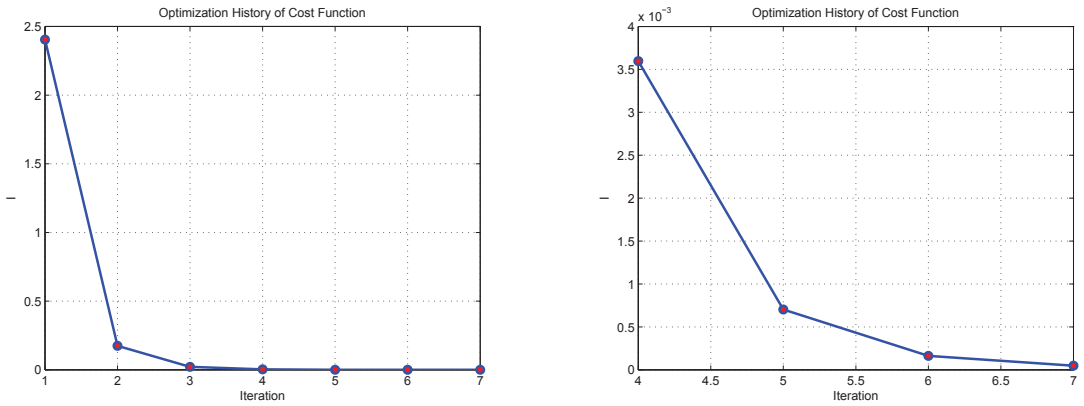

(a) Iterations 1-7 (b) Iterations 4-7

Figure 1. Convergence History of Cost Function for Linear Advection

Design Inputs

The evolution of the initial conditions is shown in figure 2. After two design cycles, the initial condition becomes almost indistinguishable from the exact initial condition.

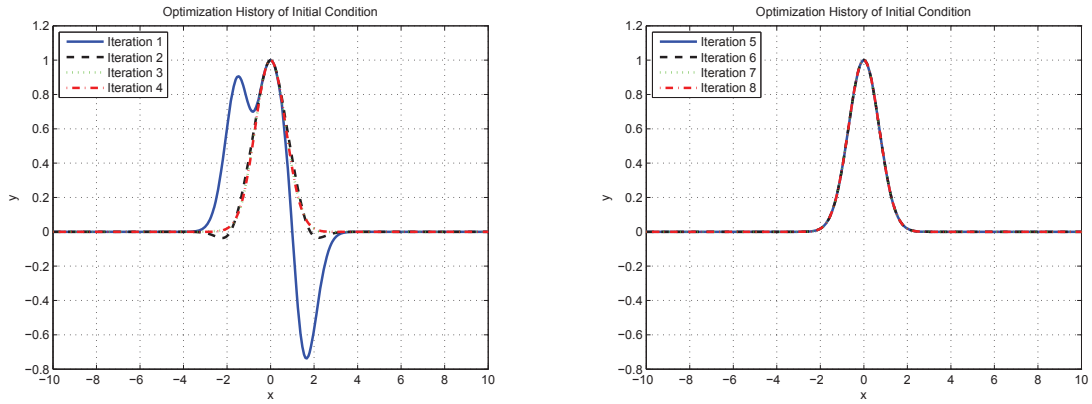

(a) Iterations 1-4 (b) Iterations 5-8

Figure 2. Optimization History of Initial Condition

Design Outputs

The final solutions are plotted in figure 3. For high order method with minimum numerical dissipation, the final solutions of the linear advection problem have almost exactly the same profiles as the initial conditions.

VI.B. Linear Inviscid Problem II

Computational Setup for Linear Advection Equation

Firstly we define the final design solution distribution, $u_d(T)$, at a specific final time, T, as before:

$$u_d(T) = e^{-20(x-cT)^2}$$

Secondly we specify an abritary initial condition, with the only requirements that no errors at the boundaries, either Dirichilet or Neumann type, are introduced. Assuming we do not know where to start, we simply set the initial condition as zero:

$$u(x, 0) = 0$$

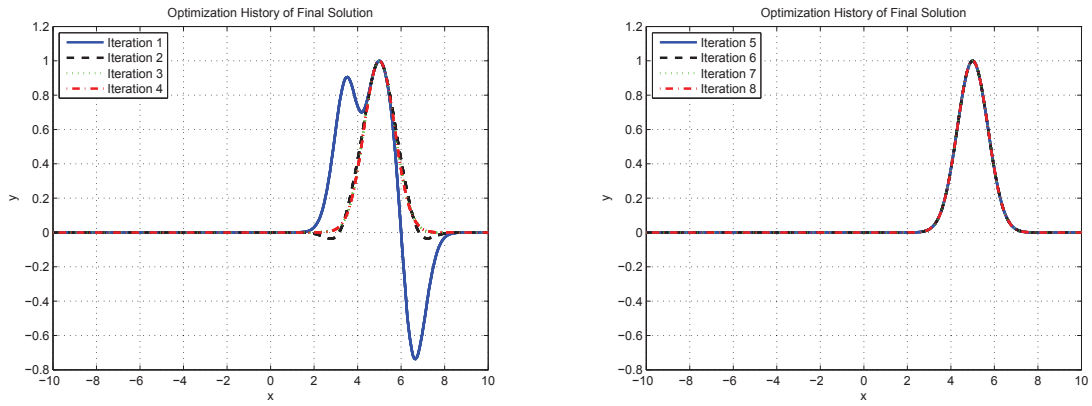

(a) Iterations 1-4 (b) Iterations 5-8

Figure 3. Optimization History of Final Solutions at Time T=5s

Design Convergence

The evolution of the cost function is shown in figure 4. It takes five iterations to reduce the cost function to the desired tolerance.

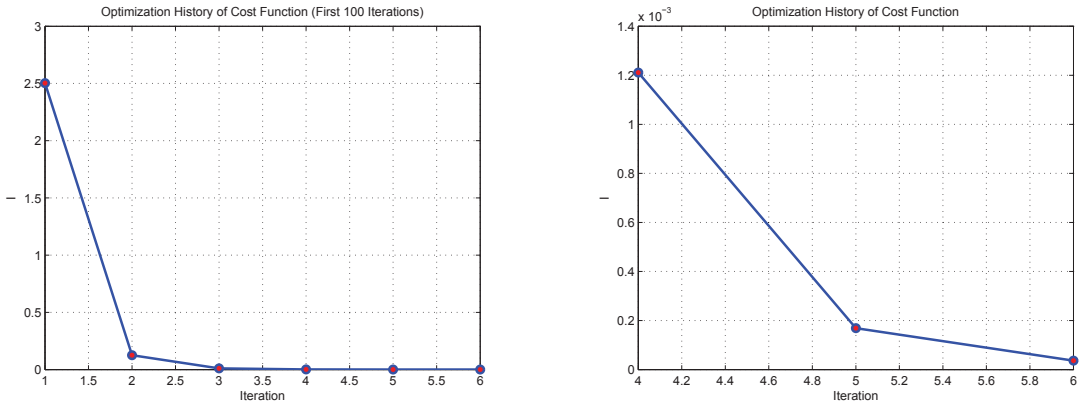

(a) Iterations 1-6 (b) Iterations 4-6

Figure 4. Optimization History of Cost Function

Design Inputs

The initial conditions at different design cycles are plotted in figure 5. As can be clearly observed, after one iteration, the exact initial condition is almost recovered.

Design Outputs

Similarly, the target solution distribution at the final time is attained in about one design iteration, as shown in figure 6.

VI.C. Viscous Non-linear Problem I

For the non-linear viscous problem, we consider the viscous Burger's equation, written as follows:

$$\frac{\partial u}{\partial t} + u\frac{\partial u}{\partial x} - \mu\frac{\partial^2 u}{\partial x^2} = 0 \tag{18}$$

Two exact solutions of viscous Burger's equation are used to illustrate the unsteady adjoint method for the optimal control of the Burger's equation.

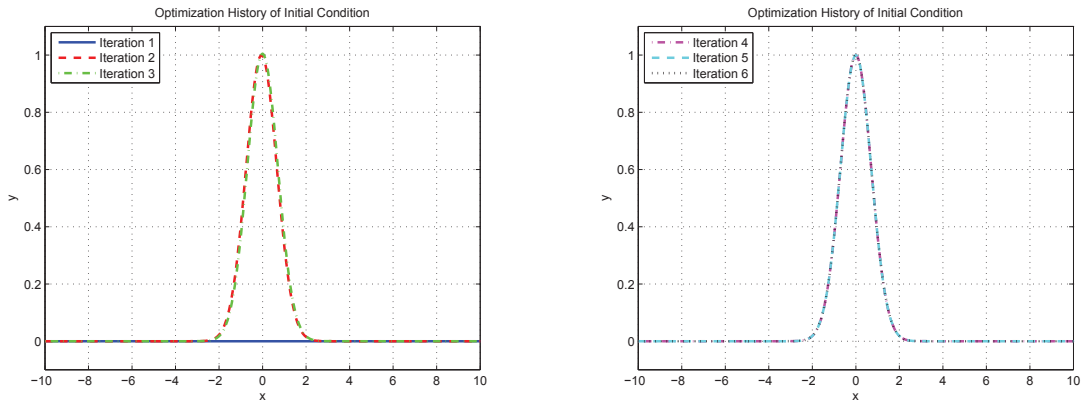

(a) Iterations 1-3 (b) Iterations 4-6

Figure 5. Optimization History of Initial Conditions

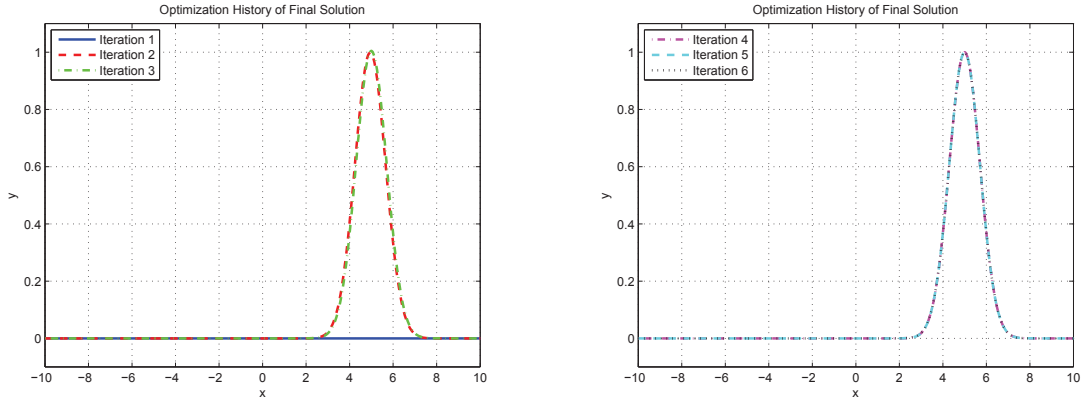

(a) Iterations 1-3 (b) Iterations 4-6

Figure 6. Optimization History of Final Solutions at Time T=5s

Computational Setup for Viscous Burger's Equation

The first exact solution[13] for the viscous Burger's equation is given by:

$$u(x,t) = \frac{2\mu\pi e^{(-\pi^2\mu t)} sin(\pi x)}{const + e^{(-\pi^2\mu t)} cos(\pi x)}$$

with the boundary conditions:

$$u_l = 0$$

$$u_r = 0$$

and the initial condition:

$$u(x,0) = \frac{2\mu\pi sin(\pi x)}{const + cos(\pi x)}$$

The computational domain spans $[-2, 2]$ with a total number of 40 elements. The number of solution points witin each element is 4, corresponding to 4^{th} order accurate SD method. The computation is run with a fixed time step of $dt = 0.005$ until a final time $T = 4$. The same time step size is used for solving the adjoint equation. The viscosity coefficien is chosen as $\mu = 0.01$. The value for the constant parameter is set to $const = 2$. The same Euclidean norm of the final error is defined as the cost function and we select the tolerance for the non-linear viscous problem to be $1E^{-3}$.

Design Convergence

Firstly we define the final design solution distribution, $u_d(T)$, at a specific final time, T, as:

$$u_d(x,T) = \frac{2\mu\pi e^{(-\pi^2\mu T)} sin(\pi x)}{const + e^{(-\pi^2\mu T)} cos(\pi x)}$$

Secondly we define the initial condition as the exact initial condition with an added error function that has a Gaussian distribution as follows:

$$u = \frac{2\mu\pi sin(\pi x)}{const + cos(\pi x)} + 0.25e^{-4x^2}$$

The convergence of the cost function is shown in figure 7. It takes about 60 design cycles to reach the design tolerance. While the actual convergence is heavily problem specific, depending on the selected viscosity, final time, initial conditions and other parameters, overall the current problem converges at a much slower rate than the linear advection problem, largely due to its inherent non-linearity and viscous dissipation. But despite the more complex nature of the current problem, the unsteady adjoint method still produces the desired solution within a small number of design cycles.

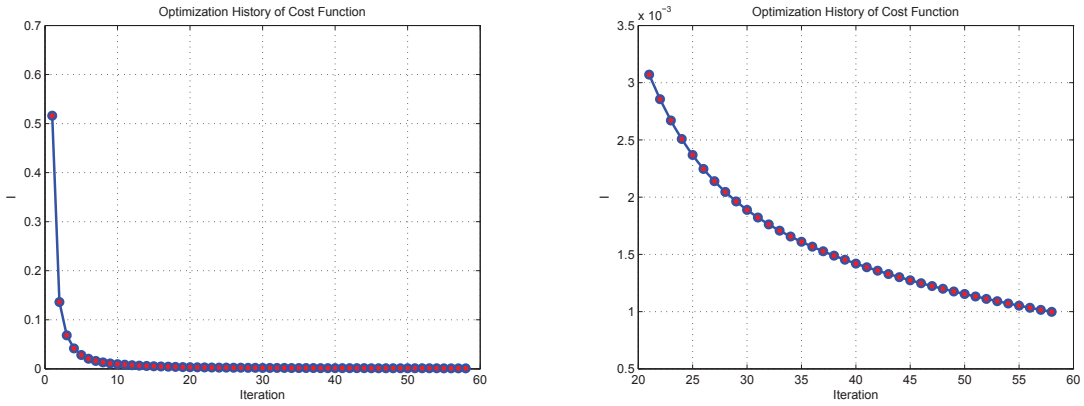

(a) Iterations 1-58 (b) Iterations 21-58

Figure 7. Optimization History of Cost Function

Design Inputs

Figure 8 shows the progressive change of the initial conditions as the optimization progresses. We observe that the magnitude of the initial input approaches the actual initial condition very quickly, but the exact matching of the profile requires much more design cycles.

Design Outputs

The design evolution of the final solution is shown in figure 9. Similarly we see fast decay of error magnitude but slow convergence of distribution profile.

VI.D. Viscous Non-linear Problem II

For the second example of non-linear viscous problem, we consider a solution of the viscous Burger's equation with shock like steep gradient.

Computational Setup for the Non-linear Viscous Burger's Equation

The exact solution for the viscous Burger's equation[14] is given by:

$$u = 0.5\left[1 - tanh(\frac{x - t/2}{4\mu})\right]$$

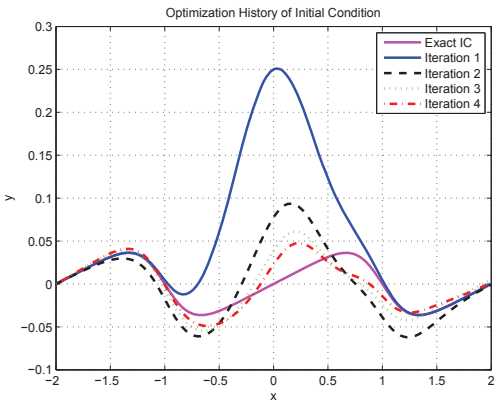

(a) Iterations 1-4

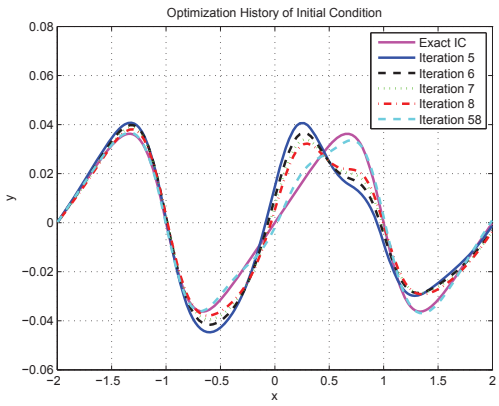

(b) Iterations 5-8 and the last iteration

Figure 8. Optimization History of Initial Condition

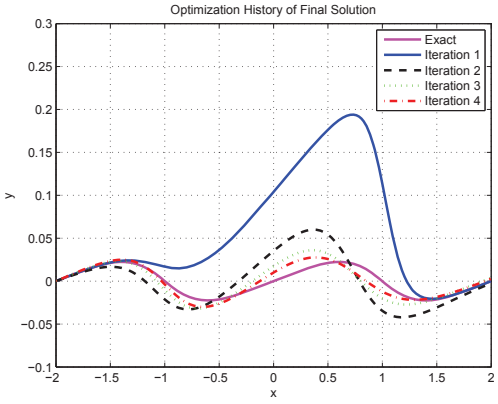

(a) Iterations 1-4

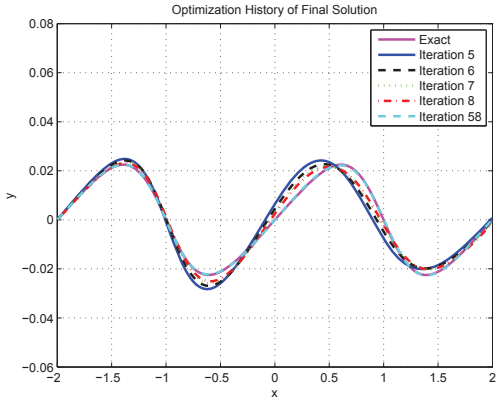

(b) Iterations 5-8 and the last iteration.

Figure 9. Optimization History of Final Solutions at Time T=4s

with the boundary conditions:

$$u_l = 0.5\left[1 - tanh(\frac{x_l - t/2}{4\mu})\right]$$

$$u_r = 0.5\left[1 - tanh(\frac{x_r - t/2}{4\mu})\right]$$

and the initial solution:

$$u_0 = 0.5\left[1 - tanh(\frac{x_0}{4\mu})\right]$$

The computational domain spans $[-5, 5]$ with a total number of 100 elements. The number of solution points witin each element is 3, corresponding to 3^{rd} order accurate SD method. The computation is run with a fixed time step of $dt = 0.005$ until a final time $T = 2$. The same time step size is used for solving the adjoint equation. The viscosity coefficien is chosen as $\mu = 0.05$, which determines the width of the discontinuity. The location of the discontinuity at time t is at $\frac{t}{2}$.

Design Convergence

Firstly we define the final design solution distribution, $u_d(T)$, at a specific final time, T, as:

$$u = 0.5\left[1 - tanh(\frac{x - T/2}{4\mu})\right]$$

Secondly we define the initial condition as a ramp function as follows:

$$u(x,0) = \begin{cases} 1.0 & x < -2.5 \\ 0.0 & x > 2.5 \\ 0.5 - 0.25x & else \end{cases}$$

The convergence of the cost function is plotted in figure 10. After 50 design cycles, the cost function is reduced to about $3E^{-2}$.

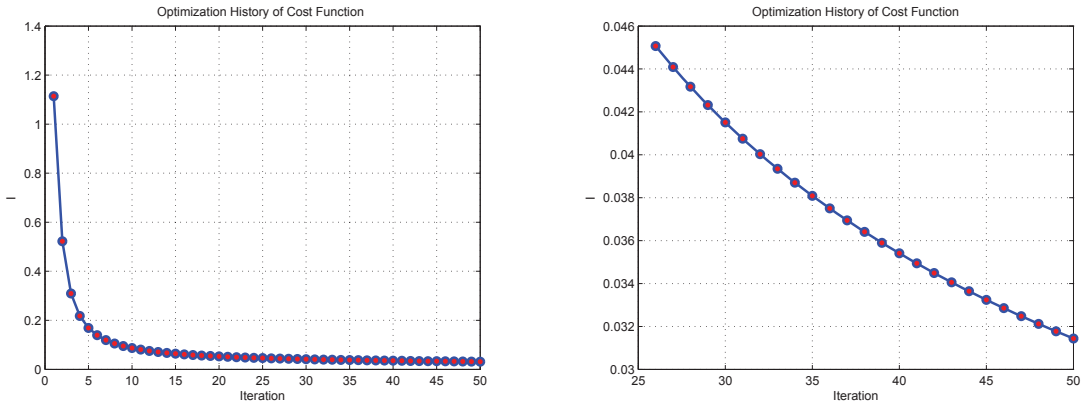

(a) Iterations 1-50 (b) Iterations 25-50

Figure 10. Optimization History of Cost Function

Design Inputs

The changes of the initial conditions are shown in figure 11. We find that the input control becomes increasingly oscillatory as it evolves from a ramp function towards the exact initial condition, which has a profile of a lightly smoothed step function. This is a sign that the optimization method attemps to represent the step like function with sinc function. Hence as the width of the discontinuity gets smaller, the matching of the exact initial condition gets increasingly more difficult.

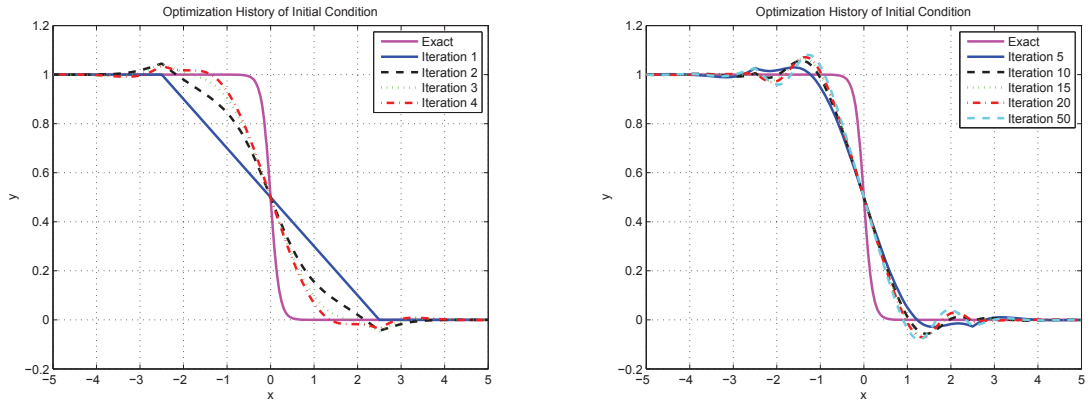

(a) Iterations 1-4 (b) Iterations 5-50

Figure 11. Optimization History of Initial Condition

Design Outputs

Even though the initial inputs do not exactly match the actual input, the final solution matches quite well with the design solution, as shown in figure 12 (b). This is evidence of the non-uniqueness of Burger's equation's solutions. Due to its non-linearity, the same solution can be reached with different initial conditions.

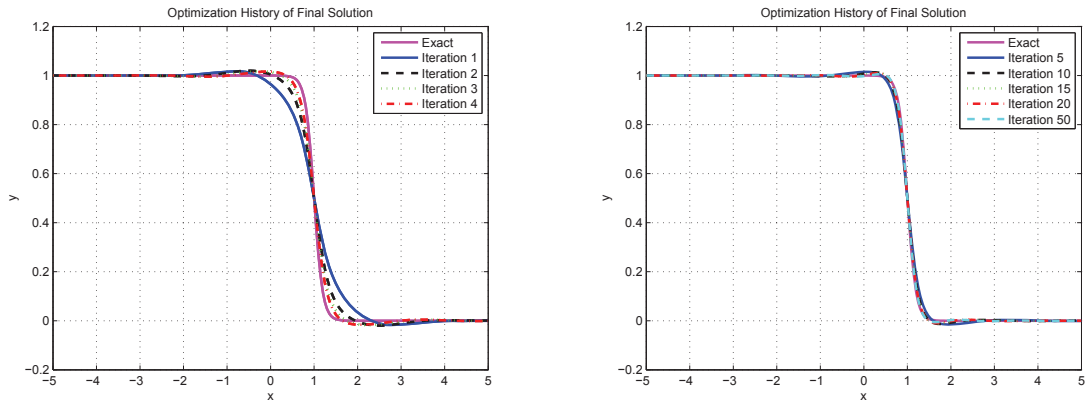

(a) Iterations 1-4 (b) Iterations 5-50

Figure 12. Optimization History of Final Solutions at Time T=2s

VI.E. Benefit of High Order Accuracy for Unsteady Adjoint Problem - Comparison with Finite Volume Method

Finally, to study the relative advantage of applying high order method, in comparison with the traditional low order method, for solving the unsteady adjoint method, we perform the computation of the same linear advection problem with a finite volume method, in the same domain $[-10, 10]$, using the same time step $dt = 0.05$ and the same total number of degrees of freedom with 400 elements.

Linear Advection Inverse Design Convergence with Finite Volume Method

The advantage of high order method for solving the unsteady adjoint problem is clearly observed from the cost function convergence plot, as shown in figure 13. After over $1,200$ design cycles, the cost function is still one order of magnitude above the specified tolerance. From the logarithmic plot of figure 13 (b), it would take an estimated $10,000$ iterations for the finite volume method to reach the tolerance of $1E^{-4}$, while from the previous section, it took only 6 design cycles (not counting the first one that is the initial iteration) to achieve the same goal - about a three order of magnitude saving in computing requirement.

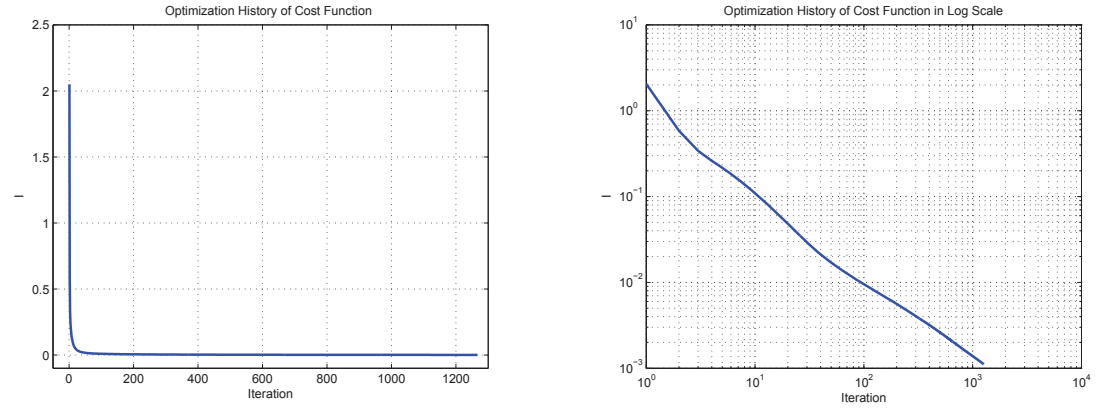

(a) Convergence history on linear scale (b) Convergence history in logarithmic scale

Figure 13. Optimization History of Cost Function

Linear Advection Inverse Design Result with Finite Volume Method

Despite having the same number of degrees of freedom in the computational domain, the numerical dissipation of the low order method has a significant effect on the optimization process. The dissipation and loss of accuracy during the wave advection process lead to wave oscillation, damping of wave magnitude and

broading of wave profile that impede the accurate and effective recovery of the final and initial conditions. To take into the account of numerical dissipation, the optimization leads to an initial input that has a similar profile but higher magnitude, as clearly seen for the initial condition on the 1000^{th} design cycle in figure 14 (b). The numerical dissiaption alone will prevent the exact recover of the initial condition, given a desired final solution.

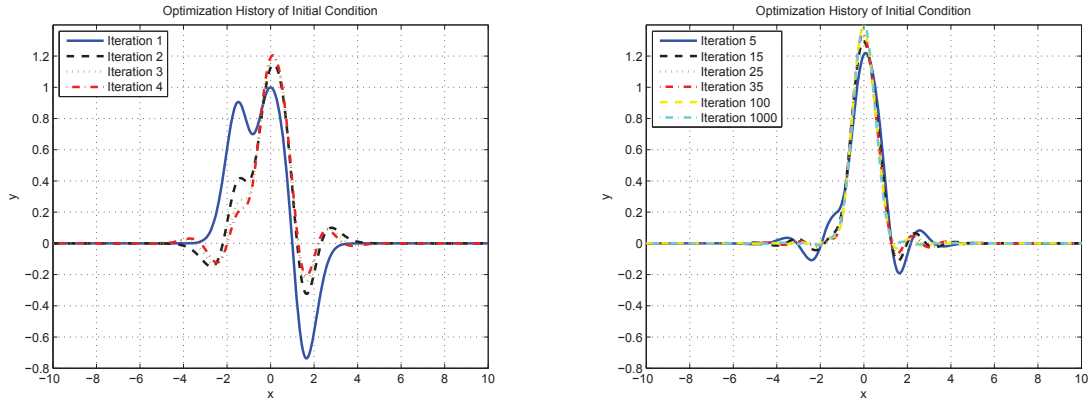

(a) Iterations 1-4 (b) Iterations 5-1000

Figure 14. Optimization History of Initial Conditions

Linear Advection Inverse Design Result with Finite Volume Method

Comparing the solution of figure 15 with the initial conditions of figure 14, the effect of numerical dissipation is clearly discernable. The same inherent disspation in the scheme will also affect the solution of the adjoint equation when it is integrated backward in time, further degrading the propogation of optimization information. As a result, the errors are removed at a much slower rate. While many more complex problems have inherent physical non-linearity and viscosity that makes the optimization converge less rapidly, as we found previously from the viscous Burger's equation for example, the minimization of numerical dissipation, however, can markedly improve the optimization and computational efficiency, and lead to better and more efficient designs at a much reduced cost.

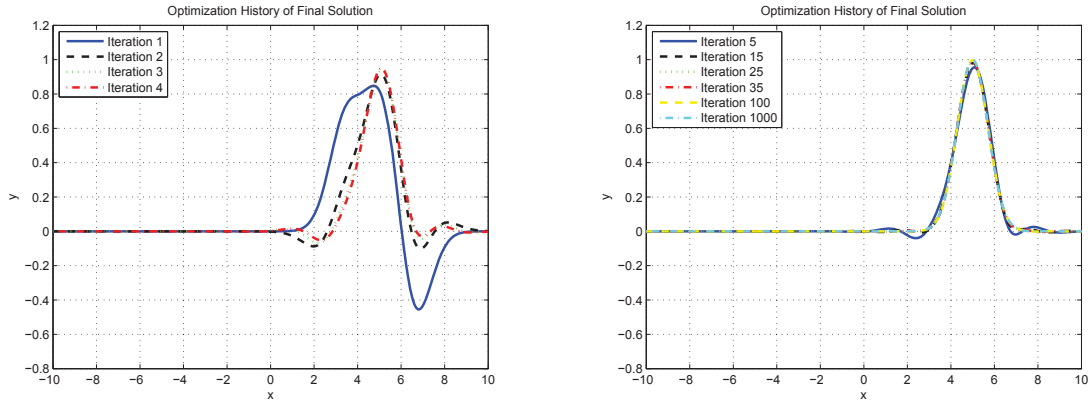

(a) Iterations 1-4 (b) Iterations 5-1000

Figure 15. Optimization History of Final Solutions at Time T=5s

VII. Conclusions

In this study, we outline the derivation of the continuous adjoint equations for both the linear advection and viscous Burger's equation, and formulate the unsteady adjoint equation using the high order spectral difference method. We present the results for the control of the linear advection and viscous Burger's

equations, and show that the design final solutions can be effectively attained through the intial condition inputs with the unsteady adjoint method. In the linear inviscid problem, this combination of high order method and adjoint method is particularly effective, achieving the design solution within only a few design iterations. Both the exact input and output can be recovered. Compared to the linear problem, the optimal control of the non-linear viscous Burger's problem requires more effort, but the effectiveness of adjoint method in driving the solution towards the design target is still clearly observed. We note that the dissipation and non-linearity prevent the exact recovery of the initial condition. This suggests that different initial conditions can lead to the same final solutions for the viscous Burger's equation, an evidence that its solutions are non-unique. Finally, we investigate the benefit of the high order unsteady adjoint method over the adjoint method discretized with the traditional low-order method. The study shows that the high order method with minimum numerical dissipation can significantly improve the optimization and computational efficiency, and lead to better and more efficient designs at a much reduced cost.

Acknowledgement

This research work is made possible by the generous fundings from the National Science Foundation and the Air Force Office of Scientific Research under the grants 0708071 and 0915006 monitored by Dr. Leland Jameson, and grant FA9550-07-1-095 by Dr. Fariba Fahroo. The authors would like to thank them for their continuous support.

References

[1]S.K.Nadarajah and A. Jameson, "Optimum Shape Design for Unsteady Flows with Time-Accurate Continuous and Discrete Adjoint Method", AIAA Journal Vol. 45, No.7, July 2007.

[2]J Reuther, A. Jameson, J. Farmer, and L. Martinelli, "Aerodynamic shape optimization of complex aircraft configurations via an adjoint formulation', 34th AIAA Aerospace Sciences Meeting and Exhibit, 1996

[3]A. Jameson, "Aerodynamic shape optimization using the adjoint method, VKI Lecture Series on Aerodynamic Drag Prediction and Reduction', von Karman Institute of Fluid Dynamics, Rhode St Genese , 2003

[4]WK Anderson, V Venkatakrishnan, "Aerodynamic design optimization on unstructured grids with a continuous adjoint formulation', 35th AIAA Aerospace Sciences Meeting and Exhibit , 1997

[5]L.Wang, D. Mavriplis, and K. Anderson, " Unsteady Discrete Adjoint Formulation for High-order Discontinuous Galerkin Discretizations in Time-dependent Flow Problems ", 48th AIAA Aerospace Sciences Meeting Including the New Horizons Forum and Aerospace Exposition, Orlando, Florida, Jan. 4-7, 2010

[6]G. Chen and S.S.Collis, "Toward optimal control of aeroacoustic flows using discontinuous Galerkin discretizations ", 42 nd AIAA Aerospace Sciences Meeting and Exhibit, 2004

[7]G. Chen and S.S.Collis, "Multimodel Methods for Optimal Control of Aeroacoustics ", 43 rd AIAA Aerospace Sciences Meeting and Exhibit, 2005

[8]Y. Sun and Z. J. Wang and Y. Liu, "High-order multidomain spectral difference method for the Navier-Stokes equations on unstructured hexahedral grids, Communication in Computational Physics, Vol. 2, pp. 310-333 (2007).

[9]Huynh, H.T., "A flux reconstruction approach to high-order schemes including discontinuous Galerkin methods", AIAA 2007-4079,18th AIAA CFD Conference, Miami, June 2008.

[10]A. Jameson, *A proof of the stability of the spectral difference method for all orders of accuracy*, J. Sci. Comput. (2010).

[11]A. Jameson and L. Martinelli, "Aerodynamic Shape Optimization Techniques Based on Control Theory", Computational Mathematics Driven by Industrial Problems, Volume 1739/2000, 151-221.

[12]S. Nadarajah and A. Jameson, "A comparison of the continuous and discrete adjoint approach to automatic aerodynamic optimization', 38th AIAA Aerospace Sciences Meeting and Exhibit, 2000

[13]W. L. Wood, "An exact solution for Burger's equation ", Communications in Numerical Methods in Engineering, Volume 22 Issue 7, Pages 797 - 798, 2006

[14]C. Castro, F. Palacios, and E. Zuazua, "Optimal Control and Vanishing Viscosity for the Burgers Equation ", Integral Methods in Science and Engineering, Volume 2 : Computational Methods.